Coalescence of Nanobranches: A New Growth Mechanism for Single Crystal Nanobelts

Weiyou Yang,*,†,‡ Zhipeng Xie,† Hezhuo Miao,† Ligong Zhang,§ and Linan An§,||

State Key Lab of New Ceramics and Fine Processing, Tsinghua University, Beijing 100084, P.R. China, School of Mechanical Engineering, Ningbo University of Technology, Ningbo 315016, P.R. China, Laboratory of Exited State Process, Changchun Institute of Optics, Fine Mechanics and Physics, Chinese Academy of Science, Changchun 130032, P.R. China, and Advanced Materials Processing and Analysis Center, University of Central Florida, Orlando, Florida 32816

Received: November 9, 2005; In Final Form: January 9, 2006

We report a fundamentally new growth mechanism for single crystalline nanobelts, namely, the growth and coalescence of nanobranches. The growth process of the nanobelts includes four typical steps such as nucleation and growth of the stem, nucleation and growth of the nanobranches at the expense of the stem, widening and geometrical coalescence of the nanobranches, and finally having nanobelts with perfect structure. The unique widening growth process of the nanobranches is apparently driven by the lattice distortion within the surface area of the stem. The continuous geometrical coalescence between the neighbored branches leads to the formation of the beltlike structures.

Introduction

The synthesis of one-dimensional nanostructured materials has attracted worldwide interest during the past few years not only because they likely possess unique properties but also because of their unique growth mechanisms.[1] Among the various nanostructures, nanobelts have caught special attention due to their unique rectangular cross-section morphology, which could lead to many potential applications. Nanobelts have been successfully synthesized in different material systems, such as B, Ni, C, ZnO, ZnS, GaN, AlN, Bi_2S_3, Ge_3N_4, Si_3N_4, et al.[2,3] The formation processes of nanobelts have also been extensively studied. While several different mechanisms such as vapor−solid (VS),[3] oxide-assisted-growth (OAG),[4] et al. were proposed, all the reported growth schemes to date have the same scenario: formation of the nuclei with rectangular-shaped cross sections followed by growth along the length direction of the nanobelts. In this paper, we report a fundamentally new mechanism for the growth of nanobelts, namely, growth and geometrical coalescence of nanobranches. This mechanism suggests the detailed growth information of nanobelts at different growth stages and assists in understanding how the rectangular-shaped cross sections are formatted.

Experimental Section

The Si_3N_4 nanostructures used in this study were synthesized by thermal decomposition of a polymeric precursor with a catalyst. The experimental procedure employed here is similar to that described previously.[5] First liquid-phased polyureasilazane was solidified into powders by heat treatment at 250 °C in flowing nitrogen for 1 h. Cu powders of ∼1 μm, used as catalyst, were mixed with the polyureasilazane powders by high-energy ball milling for 24 h. The powder mixture was then placed in a high-purity alumina crucible and heat treated in a conventional tube furnace under flowing ultrahigh purity nitrogen at 0.1 MPa. The powder mixture was heated to 1450 °C and held there for 0.5, 1, 2, and 4 h, respectively. The resulting samples were then investigated by a high-resolution transmission electron microscopy (HRTEM, JEOL-2010F, Japan) at 200 kV.

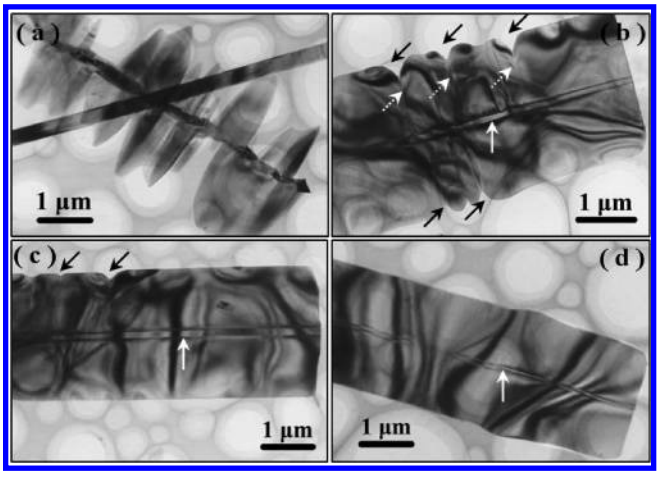

Figure 1. TEM images of the pyrolysis products obtained at holding times of (a) 0.5, (b) 1, (c) 2, and (d) 4 h, showing the growth process of the Si_3N_4 nanobelts.

Results and Discussion

The samples obtained at different holding times were first analyzed using transmission electron microscopy (TEM) to evaluate the growth process of the nanobelts. The TEM image given in Figure 1a shows the typical morphology of the product obtained at short holding time. The major product obtained at this stage is a nanodendritelike structure consisting of a wire/beltlike stem with numerous nanobranches on two opposite sides of the stem. With increasing holding time (Figure 1b), the nanobranches grew along the length direction of the stem and met with each other to form boundaries (as indicated by white dotted arrows) and notches at the end of the boundaries (as

* Corresponding author e-mail address: ywy01@mails.tsinghua.edu.cn.
† Tsinghua University.
‡ Ningbo University of Technology.
§ Chinese Academy of Science.
|| University of Central Florida.

10.1021/jp0565047 CCC: $33.50
Published on Web 02/10/2006

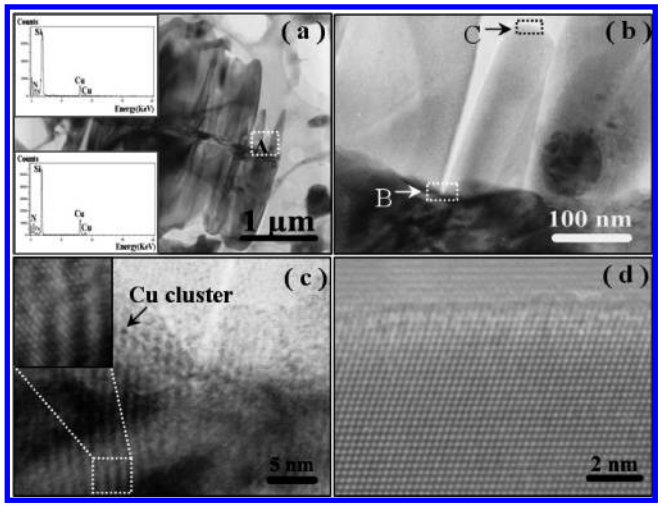

Figure 2. Structure of the nanobelts at the early growth stage. (a) Bright-field TEM image of the nanobelts. The upper left and lower left inserts corresponding to the typical EDS images were obtained from the nanobranch and stem, respectively. (b) Enlarged TEM image of the area A marked in part a. (c) HRTEM image of area B marked in part b with the insert being the enlarged HRTEM image of a selected area showing the lattice image, showing the distortion of lattice of the stem as well as a possible Cu cluster at the root of the branches. (d) HRTEM image of area C marked in part b.

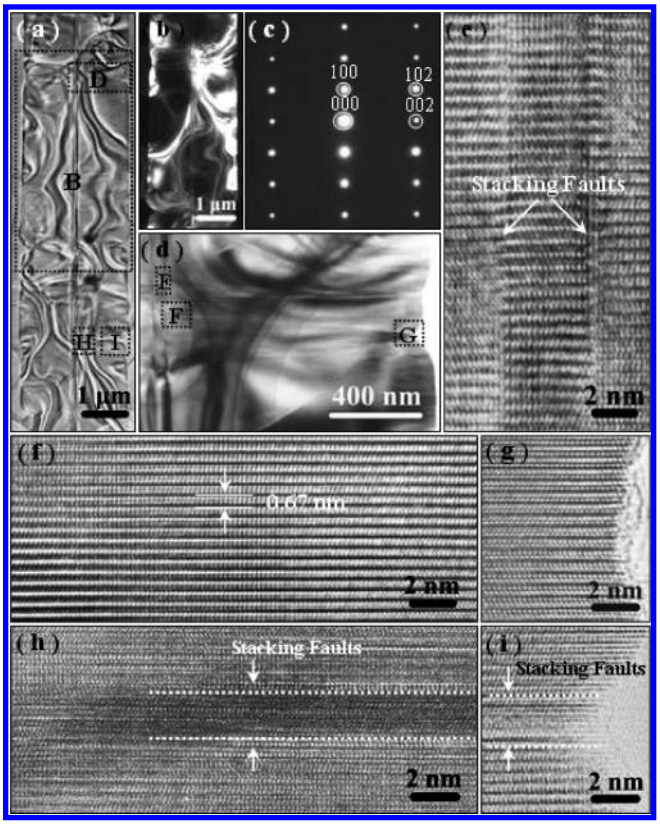

Figure 3. Structure of the nanobelts at a late stage of growth. (a) Bright-field TEM image of the nanobelt. (b) Dark-field TEM image recorded from area B marked in part a. (c) Typical SAED pattern of the nanobelts indicating that the nanobelts possess an α-Si_3N_4 structure. The SAED patterns obtained from different areas of the nanobranches and stem are identical, suggesting the single crystalline nature of the nanobelts. (d) Enlarged image of the nanobelt corresponding to the selected area D in part a. (e) HRTEM image recorded from area E as marked in part d. (f and g) HRTEM images obtained from areas F and G as marked in part d, respectively, showing the boundary area between two neighboring branches before complete combination. (h and i) HRTEM images obtained from areas H and I as marked in part a, respectively, showing the boundary area between two neighboring branches nearing complete combination with a notch.

indicated by black arrowheads). The number of such boundaries and notches were gradually reduced with holding time (Figure 1c), suggesting merging of the different nanobranches. Finally, all the boundaries and notches disappeared and seamless nanobelts with a uniform thickness were formed by extending the holding time for 4 h (Figure 1d). It can also be seen that the size of the stem (indicated by white arrows) continuously reduced during growth, indicating that the growth of the nanobranches occurred by consuming the stem. The resultant nanobelts have a large width-to-thickness ratio with typically ~40 nm in thickness, 2−3 μm in width, and up to several hundred micrometers in length. These images clearly demonstrate that the nanobelts reported here were formed by the growth and merging of nanobranches, instead of by epitaxial growth of nuclei as reported previously.

The growth manner illustrated in Figure 1 is new and interesting. Growth of structures with nanobranches (so-called nanodendrites) has been observed previously in many material systems.[6] In these previous studies, the branches always grew longer along the direction perpendicular to the length direction of the stem to form a featherlike morphology. In contrast, the nanobranches in the current study grew parallel to the length direction of the stem. Another interesting issue is how these branches merged together to form seamless beltlike structures (even without stacking faults, as discussed below in Figure 3c and 4). To further understand these issues, detailed analysis of different growth stages was carried out using TEM and high-resolution TEM (HRTEM).

Figure 2a shows the TEM image recorded from the nanobelts at an early stage of growth. The contrast suggests that different nanobranches exhibit different thickness. The different contrast between the center and edge of some nanobranches indicates that the thickness within the same nanobranch is also not uniform at this stage. The typical energy-dispersive spectrometry (EDS) images obtained from the nanobranch and stem, respectively, were given as the upper left and lower left inserts in Figure 2a, showing that both the nanobranch and stem consisted of Si and N elements only (Cu originates from the copper grid). Figure 2b is a higher magnification TEM image recorded from the root area that connects the stem and the nanobranches (area A marked in Figure 2a). The darker contrast of the stem suggests that the stem is much thicker than the nanobranches at this stage. Figure 2c is an HRTEM image recorded from area B marked in Figure 2b; the insert in Figure 2c is an enlarged image from the outlined area. These images clearly reveal that the lattice of the stem is highly distorted. Such lattice distortion existed all along the 30 nm top layer thickness of the entire stem. Some dark spots were observed at the root of the branches, as indicated by an arrow. These tiny clusters, a few tenths of a nanometer in size, may correspond to tiny Cu clusters. The distortion of the lattice and the Cu clusters suggests that there is an enrichment of Cu at the surface layer of the stem. Such an enrichment in nanostructures was not observed when Fe was used as a catalyst,[7] where nanodendrites instead of nanobelts were formed. Figure 2d shows a typical HRTEM image of the branches. The entire branch except for the area close to the root possesses perfect crystal structure with very few defects, and there is no amorphous layer on the surface of the nanobranches.

The microstructure of the nanobelts at a late stage of growth is shown in Figure 3a (TEM bright-field image) and b (TEM dark-field image). At this stage, the nanobranches formed in the early stage were found to join together leaving boundaries and notches. The selected area electron diffraction (SAED)

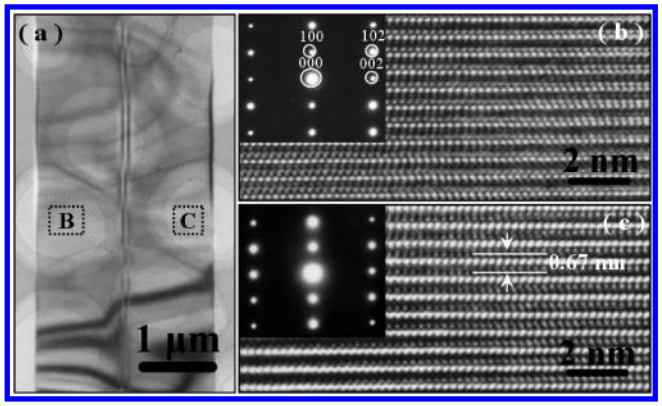

Figure 4. Typical structure of the nanobelts at the final growth stage. (a) Bright-field TEM image of the nanobelt. (b−c) HRTEM images showing the perfect and identical crystal structures on the two sides of the middle stripe.

pattern (Figure 3c) suggests that the nanobelts have α-Si_3N_4. The pattern also reveals that the length direction of the stem is along [100] and the nanobranches formed on ±(001) surfaces of the stem. The nanobranches grew along [100], instead of [001] which is preferred by the hexagonal structure of α-Si_3N_4 when there is no constraint.[8] Such an unusual growth manner of the nanobranches is likely driven by the lattice strain energy resulting from the lattice distortion in the stem. Generally, Si_3N_4 has a higher surface energy along (001) (the basal plane) than along (100) (the prism plane); thus, the material preferably grows along the [001] direction to minimize the total energy by minimizing the total surface area of the (001) plane.[8] In the present case, the strain energy arising from the lattice distortion far exceeded the energy difference between different planes; thus, the nanobranches preferentially grew along the surface of the stem to release the strain energy by removing the lattice distortion (Figure 3e). Compared to our previous study,[7] the nanodendrites were formed by using a process similar to that in the current investigation except that $FeCl_2$ was used as the catalyst. In that study, no Fe solution or lattice distortion were detected within the Si_3N_4 stem and the nanobranches grew longer along the preferred [001], which is perpendicular to the length direction of the stem. While the difference between Cu and Fe in terms of dissolution and segregation in Si_3N_4 is unknown, the results suggest that the growth behavior of nanobranches is very sensitive to the type of catalyst used, indicating a possibility of controlling the morphology of nanostructures.

It can also be seen (Figure 3a) that at this later growth stage the thickness of different nanobranches became relatively uniform and close to that of the stem. The growth of the nanobranches along the thickness direction of the stem, which could also occur due to lattice distortion, was likely constrained by the thickness of the stem. A relatively large amount of wrinklelike contrast could be seen in the images (Figure 3a and b). Such contrast is caused by bending resulting from slight lattice mismatch and/or thickness difference between different branches. Figure 3d is the enlarged picture of the selected area D marked in Figure 3a. Figure 3e is an HRTEM image of area E marked in Figure 3d. The image shows that both the stem and the branch possess perfect crystalline structure and that the preexisting lattice distortion in the stem was removed. Between the stem and the branches, there is a narrow intermediate layer (~3 nm), which connects the stem and the nanobranches via stacking faults.

The formation of nanobelts by merging the nanobranches is a direct result from the so-called "grain coalescence". Figure 3f−i shows two types of boundaries/notches at different combination stages. Figure 3 parts f and g are HRTEM images of boundaries at an early combination stage. The boundary area (~2 nm thick) between two branches can be clearly seen, as indicted by the dotted lines. Such a boundary runs through the entire belt from bottom to top. The images also reveal that there is a slight difference in the lattice patterns between the branches and boundary area; thus, the boundary energy should be very low. Figure 3 parts h and i are HRTEM images recorded from the area that was a boundary previously. While the notch can still be seen (Figure 3i), the preexisting boundary disappeared. Observations reveal that there are only two situations: either the boundary runs from bottom to top or the preexisting boundary totally disappears. Such results suggest that the combination of branches is achieved by geometrical coalescence, in which a low energy boundary can be removed suddenly through atom rearrangement.[9] Such a mechanism occurs in the current study and is likely due to the high synthesis temperature and low boundary energy.

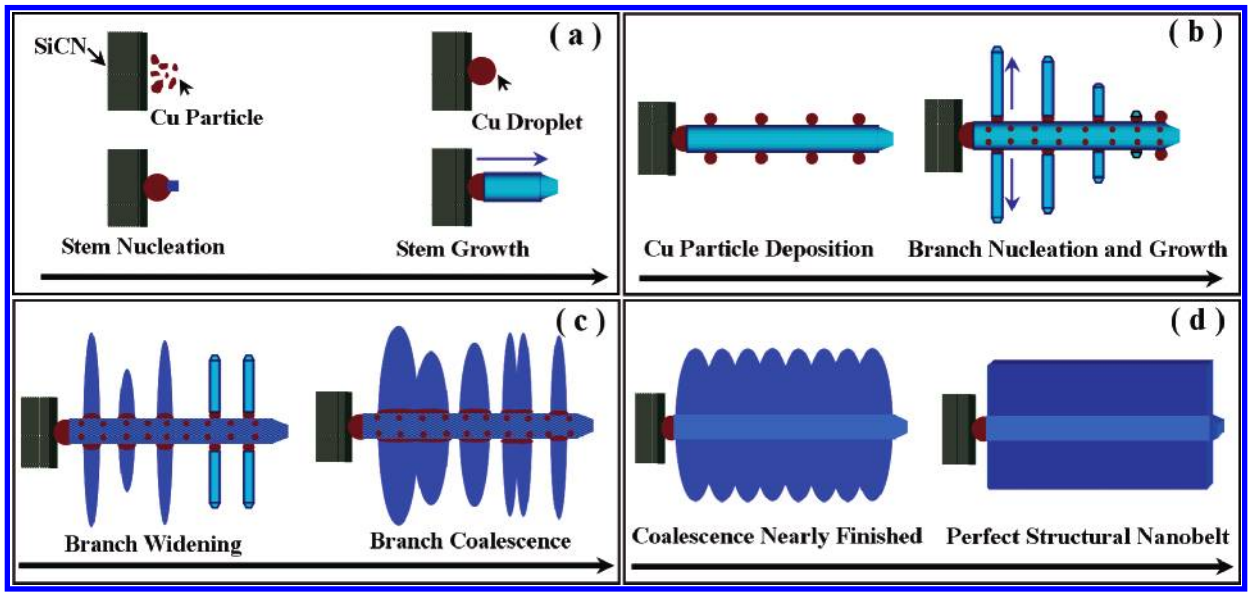

Figure 5. Model for the nanobelts growth via the mechanism of growth and coalescence of nanobranches. (a) Stem nucleation and growth. (b) Branch nucleation and growth. (c) Branch widening growth followed by geometrical coalescence. (d) Resulting perfectly structured nanobelts.

Figure 4 shows the typical structure of the final nanobelts. No notch can be seen from the image (Figure 4a), suggesting that the notch formed at an earlier stage was removed by surface diffusion. It can also be seen that the strain-induced contrast is much less than that in Figure 3a and b. Figure 4 parts b and c are the typical HRTEM images recorded from both the sides of the nanobelts with the corresponding SAED patterns recorded from the selected areas of B and C marked in Figure 4a, which showed that the crystal structures were identical on the two sides of the middle stripe. No planar defects are found over the two sides of the nanobelt, suggesting the perfect crystal structure of the nanobelts.

On the basis of the above analysis, a model is proposed for the growth of nanobelts via the mechanism of growth and coalescence of nanobranches, as shown in Figure 5. The process includes four typical steps. First, the stems nucleate and grow via the mechanism of solid−liquid−gas−solid (SLGS) (Figure 5a).[10] Second, the nanobranches nucleate and grow at the expense of the stem (Figure 5b). The Cu particles evaporated in the atmosphere would deposit on the newly grown stem and act as new nucleation sites for the growth of nanobranches perpendicular to the growth direction of the stem via the mechanism of SLGS. At the same time, some Cu atoms would precipitate to the surface layer of the stem and result in the distortion of the lattice. Third, the nanobranches are driven by the distortion energy to grow parallel along the axial direction of the stem and lead to the widening growth of the nanobranches. The geometrical coalescence between two neighbored branches would happen when the branches met each other, as shown in Figure 5c. Such widening and geometrical coalescence between two neighboring branches would continue to minimize the distortion energy until all the branches disappeared completely. Finally, nanobelts with the perfect structure would be achieved. The remaining notches on the two sides of the nanobelts would be removed by surface diffusion.

Conclusion

In summary, we report a new growth mechanism for nanobelts: growth and coalescence of nanobranches. The widening growth of nanobranches along the length direction of the stem instead of along the axes of the branches is driven by lattice distortion that existed within the surface area of the stem. The complete disappearance of the boundaries between the neighboring branches is through continuous geometrical coalescence. It is likely that such a mechanism can be used to grow nanobelts in various material systems by a proper choice of the catalyst. Unlike the conventional growth mechanisms where the aspect ratio of nanobelts is limited by anisotropic growth along different crystalline directions, the new mechanism could lead to nanobelts of high aspect ratios, which is potentially useful in many applications such as nanosubstrates.

Acknowledgment. The authors are thankful for support from the National Natural Science Foundation of China (Grant No. 50372031), the Specialized Research Fund for the Doctoral Program of Higher Education (Grant No. 20050003004), and the "Hundred Person" program of the Chinese Academy of Science. We also thank Profs. Yuan J. (TU) and Suryanarayana C. (UCF) for helpful discussion.

References and Notes

(1) Xia, Y.; Yang, P.; Sun, Y.; Wu, Y.; Mayers, B.; Gates, B.; Yin, Y.; Kim, F.; Yan, H. *Adv. Mater.* **2003**, *15*, 353.

(2) (a) Xu, T.; Zheng, J.; Wu, N.; Nicholls, A. W.; Roth, J. R.; Dikin, D. A.; Ruoff, R. S. *Nano Lett.* **2004**, *4*, 963. (b) Yin, L.; Bando, Y.; Zhu, Y.; Li, Y. *Appl. Phys. Lett.* **2003**, *83*, 3584. (c) Liu, J.; Shao, M.; Tang, Q.; Zhang, S.; Qian, Y. *J. Phys. Chem. B* **2003**, *107*, 6329. (d) Jiang, Y.; Meng, X.; Liu, J.; Xie, Z.; Lee, C.; Lee, S. *Adv. Mater.* **2003**, *15*, 323. (e) Liu, Z.; Peng, S.; Xie, Q.; Hu, Z.; Yang, Y.; Zhang, S.; Qian, Y. *Adv. Mater.* **2003**, *15*, 936. (f) Bae, S.; Seo, H.; Park, J.; Yang, H.; Park, J.; Lee, S. *Appl. Phys. Lett.* **2002**, *81*, 126. (g) Liu, Z.; Li, S.; Yang, Y.; Peng, S.; Hu, Z.; Qian, Y. *Adv. Mater.* **2003**, *15*, 1946. (h) Gao, Y.; Bando, Y.; Sato, T. *Appl. Phys. Lett.* **2001**, *79*, 4565. (i) Wu, Q.; Hu, Z.; Wang, X.; Chen, Y.; Lu, Y. *J. Phys. Chem. B* **2003**, *107*, 9726. (j) Wang, X.; Ding, Y.; Summers, C. J.; Wang, Z. *J. Phys. Chem. B* **2004**, *108*, 8773.

(3) Pan, Z.; Dai, Z.; Wang, Z. *Science* **2001**, *291*, 1947.

(4) Zhang, R.; Lifshitz, Y.; Lee, S. *Adv. Mater.* **2003**, *15*, 635.

(5) Yang, W.; Miao, H.; Xie, Z.; Zhang, L.; An, L. *Chem. Phys. Lett.* **2004**, *383*, 441.

(6) (a) Cao, L.; et al. *Adv. Mater.* **2002**, *14*, 1294. (b) Ma, R.; Bando, Y.; Sato, T.; Bourgeois, L. *Diamond Relat. Mater.* **2001**, *11*, 1397. (c) Jian, J.; Chen, X.; Wang, W.; Dai, L.; Xu, Y. *Appl. Phys. A* **2003**, *76*, 291. (d) Zhu, Y.; Hu, W.; Hsu, W.; Terrones, M.; Grobert, N.; Hare, J.; Kroto, H. W.; Walton, D. R. M.; Terrones, H. *Chem. Phys. Lett.* **1999**, *309*, 327. (e) Kuang, D.; Xu, A.; Fang, Y.; Liu, H.; Frommen, C.; Fenske, D. *Adv. Mater.* **2003**, *15*, 1747. (f) Wang, Z.; Kong, X.; Zuo, J. *Phys. Rev. Lett.* **2003**, *91*, 185502-1.

(7) Yang, W.; Xie, Z.; Li, J.; Miao, H.; Zhang, L.; An, L. *Solid State Commun.* **2004**, *132*, 263.

(8) Perera, D. S.; Mitchell, D. R. G.; Leung, S. *J. Eur. Ceram. Soc.* **2000**, *20*, 789.

(9) Nielsen, J. P. *Recrystallization, grain growth and texture*; ASM Seminar Series; American Society for Metals: Metals Park, Ohio, 1966; p 141.

(10) Yang, W.; Xie, Z.; Miao, H.; Ji, H.; Zhang, L.; An, L. *J. Am. Ceram. Soc.* **2005**, *88*, 466.